Available online at www.sciencedirect.com
ScienceDirect
Journal of the European Ceramic Society 27 (2007) 4287–4290
www.elsevier.com/locate/jeurceramsoc

Electrical properties of the $Sr_2Ru_{1-x}Ti_xO_4$ solid solutions

K. Miwa [a], I. Kagomiya [a], H. Ohsato [a,*], H. Sakai [b], Y. Maeda [b]

[a] *Department of Materials Science and Engineering, Graduate School of Engineering, Nagoya Institute of Technology, Gokiso-cho, Showa-ku, Nagoya 466-8555, Japan*
[b] *KOA corporation, Minowa-machi, Kamiina-gun, Nagano 399-4697, Japan*

Available online 23 May 2007

Abstract

The $Sr_2Ru_{1-x}Ti_xO_4$ solid solution with the K_2NiO_4-type structure has been prepared by a conventional solid-state reaction method. The lattice constants of $Sr_2Ru_{1-x}Ti_xO_4$ refined by the whole-powder-pattern-decomposition (WPPD) method have increased *a*-axis and decreased *c*-axis with the substitution of Ti^{4+} for Ru^{4+}. The change from metal to semi-conducting behavior has been confirmed between $x = 0.2$ and 0.4. Seebeck coefficient Q is positive for $x = 0$, 0.2, 0.4, 0.6 and 0.8. In addition, a large difference of Seebeck coefficient has been observed below 326.84 °C between $x = 0.4$ and 0.6. The electronic states of Sr_2RuO_4 have been covered to the Ru 4d state surrounding of Fermi level widely calculated by DV Xα method. The energy band gap of Sr_2TiO_4 have observed between the O 2p state and Ti 3d state. The experimental conductive behavior has been supported by DV Xα simulation results.

Keywords: The $Sr_2Ru_xTi_{1-x}O_4$ solid solution; X-ray methods; Electrical properties; Thermal properties

1. Introduction

The electrical properties of A_2BO_4 (B = transition metal ion), K_2NiO_4-type structure, have been well investigated for many applications such as electrodes, sensors, magnetism, optics, etc.[1–3] This structure possesses ABO_3 (B = transition metal ion), perovskite-type, layers between rock-salt A–O layers, B–O–B interactions occurring only in the *ab* plane have been investigated.[4] The K_2NiF_4-type structure; Sr_2RuO_4 has also been investigated as a spin-triplet unconventional superconductor with $T_c \sim -271.66$ °C.[5] Recently, it has been reported that the $Sr_2Ru_{1-x}Ti_xO_4$ solid solution, with the substitution of non-magnetic Ti^{4+} ($3d^0$) for Ru^{4+} ($4d^4$) in Sr_2RuO_4, changes from spin-triplet superconductivity to magnetic ordering for $x \geq 0.25$.[6,7] Polycrystalline samples of $Sr_2Ru_{1-x}Ti_xO_4$ with composition $0 \leq x \leq 1$, on the other hand, have been synthesized and the electrical resistivities determined at room temperature.[8] The electrical resistivities above room temperature, however, have not been clarified yet. In the perovskite-type $SrRu_{1-y}Ti_yO_3$ solid solution, it has been reported that a cubic to orthorhombic transition and a change from metal to semi-conducting behavior occurs between $y = 0.40$ and 0.50.[9] In this study, structural and thermal electric properties for the $Sr_2Ru_{1-x}Ti_xO_4$ solid solution were evaluated to clarify the relationship of both properties. In addition, the experimental results were supported by the calculation of electronic states of the end-members for $Sr_2Ru_{1-x}Ti_xO_4$ using the first-principles DV Xα method.

2. Experimental

All samples were prepared by solid-state reaction method: stoichiometric amounts of strontium carbonate, ruthenium dioxide and titanium dioxide were weighed out composition in the following stoichiometries, $x = 0$, 0.2, 0.4, 0.6, 0.8 and 1.0, and wet mixed for 24 h. The dried mixture was then calcined at 1000 °C for 24 h in air. These calcined powders were grounded and pressed into pellets with diameter, 12 mm. Subsequently the pellets were sintered at 1350 °C for 24 h.[8]

Structural phase identification was conducted using X-ray powder diffraction with an X'pert system using Cu Kα radiation. The lattice constants were refined by the whole-powder-pattern-decomposition (WPPD) program.[10] The thermal electric properties, resistivity ρ and the Seebeck coefficient Q, were measured in a vacuum using the four-point DC method from room temperature to 499.84 °C. Electrical contacts were made with thin platinum wires and silver paint. First-principles molecular orbital (MO) calculations were executed by the discrete variational Xα (DV Xα) method using program code SCAT[11] in order

* Corresponding author.
E-mail address: ohsato@mse.nitech.ac.jp (H. Ohsato).

0955-2219/$ – see front matter © 2007 Elsevier Ltd. All rights reserved.
doi:10.1016/j.jeurceramsoc.2007.02.146

Table 1
Structural information for Sr_2RuO_4 and Sr_2TiO_4 calculated using the DV Xα calculation (a) Sr_2RuO_4; (b) Sr_2TiO_4

Atom	Valence state	Wyckoff letter	x	y	z
(a) Sr_2RuO_4, $a=3.871$; $c=12.702$					
Sr	2	4e	0	0	0.3538
Ru	4	2a	0	0	0
O(1)	−2	4c	0	0.5	0
O(2)	−2	4e	0	0	0.1630
Atom	Valence state	Wyckoff letter	x	y	z
(b) Sr_2TiO_4, $a=3.884$; $c=12.6$					
Sr	2	4e	0	0	0.355
Ti	4	2a	0	0	0
O(1)	−2	4c	0	0.5	0
O(2)	−2	4e	0	0	0.152

to obtain the electronic states. The atomic positions in this study are given in Table 1. They were generated and optimized by solving the radial part for a given environment at each iteration of the self-consistent calculation. $[Sr_8M_5O_{42}]^{-48}$ (M = Ti, Ru) cluster models were used for the calculations as shown in Fig. 1. The cluster models assumed a coordination number 9 for Sr^{2+} and 6 for M^{4+}. In addition, a transition metal ion was replaced in center position of the cluster. The Madelung field was applied over a large volume in order for atoms at edge to have an electrostatic environment similar to that of the core atoms, a Madelung field of 545 atoms was applied.

3. Result and discussion

3.1. The structural study

The XRD patterns show that the series forms a solid solution with the K_2NiO_4-type structure. The composition dependence of the lattice constant of $Sr_2Ru_{1-x}Ti_xO_4$ refined by the WPPD method is shown in Fig. 2. With the substitution of Ti^{4+} for Ru^{4+}, the lattice constants exhibit an increased a-axis, decreased c-axis and cell volume. Due to the last that the ionic radius of Ti^{4+} ($r=0.605$ Å, 6CN) is slightly smaller than that of Ru^{4+} ($r=0.620$ Å 6CN). Although the perovskite-type $SrRu_{1-y}Ti_yO_3$ solid solution shows a clear transition from cubic to orthorhombic between $y=0.40$ and 0.50, the structural variation of $Sr_2Ru_{1-x}Ti_xO_4$ is not confirmed since there is only a slight variation of lattice constant. It is considered that crystal structures of the end-members for $Sr_2Ru_{1-x}Ti_xO_4$ are more similar than these of $SrRu_{1-y}Ti_yO_3$.

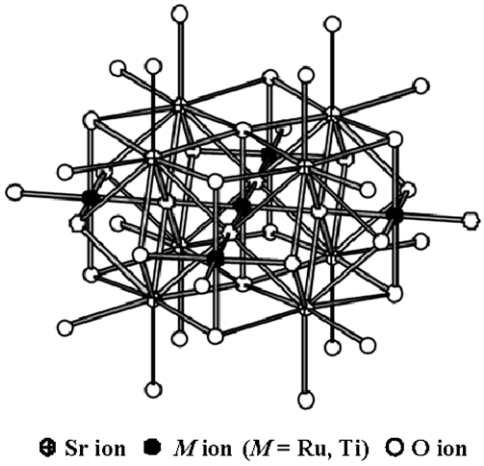

Fig. 1. $[Sr_8M_5O_{42}]^{-48}$ cluster models (M = Ru, Ti) prepared for the DV Xα calculation.

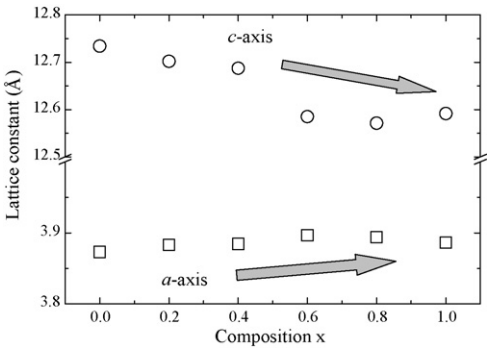

Fig. 2. Lattice constants of the $Sr_2Ru_{1-x}Ti_xO_4$ solid solution refined by the WPPD method.

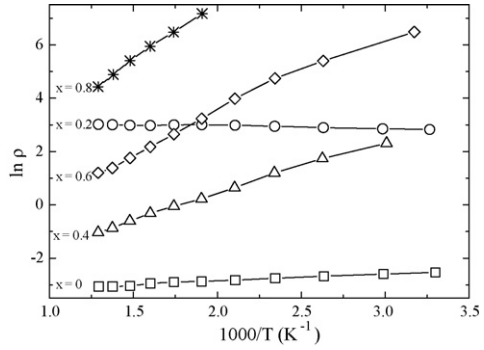

Fig. 3. Arrhenius plots of electrical resistivity ρ for the $Sr_2Ru_{1-x}Ti_xO_4$ solid solution measured from room temperature to 453.84 °C.

3.2. Thermal electric properties of resistivity and Seebeck coefficient

Fig. 3 shows the temperature dependence of the electrical resistivity, which was measured from room temperature to

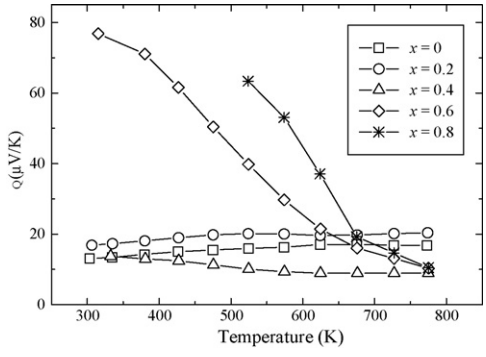

Fig. 4. Seebeck coefficient, Q, of the $Sr_2Ru_{1-x}Ti_xO_4$ solid solution measured from room temperature to 453.84 °C.

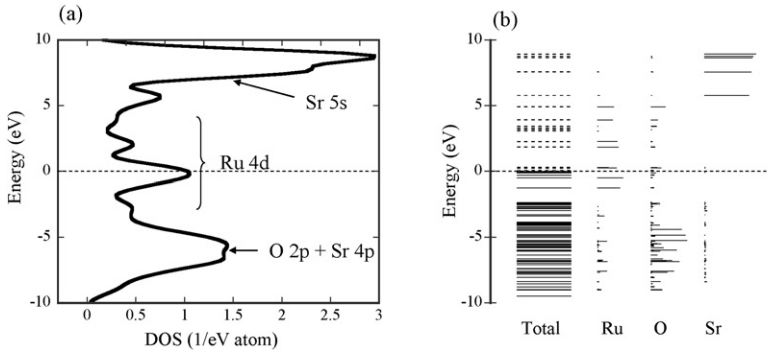

Fig. 5. The electronic state diagrams of $[Sr_8Ru_5O_{42}]^{-48}$ cluster model calculated by the DV Xα method. (a) Density of state (DOS); (b) energy level.

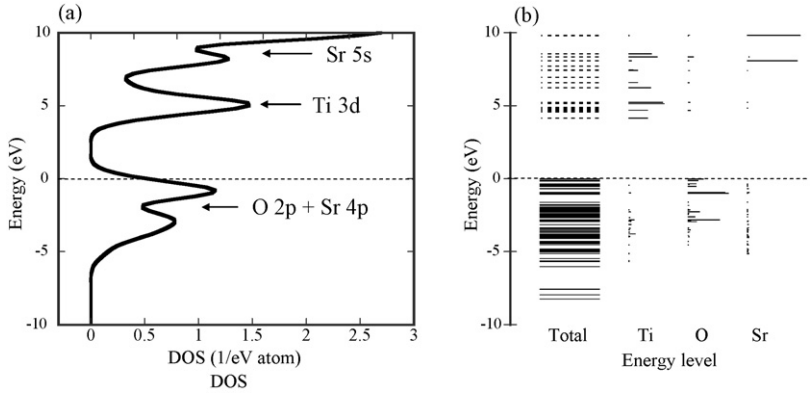

Fig. 6. The electronic state diagrams of $[Sr_8Ti_5O_{42}]^{-48}$ cluster model calculated by the DV Xα method. (a) Density of state (DOS); (b) energy level.

499.84 °C for the $Sr_2Ru_{1-x}Ti_xO_4$ with $x = 0$, 0.2, 0.4, 0.6 and 0.8. Although the compounds in $0 \leq x \leq 0.2$ exhibit metallic behavior, in $0.4 \leq x \leq 0.8$ semi-conducting behavior is exhibited. In addition, the resistivity of Sr_2RuO_4 ($x = 0$) is several orders of magnitude lower than that of $Sr_2Ru_{0.8}Ti_{0.2}O_4$ ($x = 0.2$). The compound Sr_2TiO_4 ($x = 1.0$) is an insulator. The change from metal to semi-conducting behavior for the $Sr_2Ru_{1-x}Ti_xO_4$ occurs between $x = 0.2$ and 0.4. This metal-semi-conducting transition range coincides with the transition range from spin-triplet superconductivity to magnetic ordering between $x = 0.125$ and 0.25.[6] Both transitions are likely to be related. The Seebeck coefficient Q, on the other hand, is positive for all samples as shown in Fig. 4. In addition, a large difference of Q in low temperature range was observed between $x = 0.4$ and 0.6. It is considered that the appearance of a superstructure with insulating and conducting B–O–B layers in A_2BO_4 K_2NiO_4-type structure occurs as substitution of Ti^{4+} for Ru^{4+} near room temperature. Similar behavior has been observed in $RuSr_2GdCu_2O_8$.[12]

3.3. First-principle MO calculation by the DV Xα method

The electronic state diagrams for Sr_2MO_4 (M = Ru, Ti) shown in Figs. 5 and 6 were obtained by first-principle calculation using the DV Xα method. The diagrams were plotted as Fermi level to 0 eV. The electric state diagrams of Sr_2RuO_4 were covered to the Ru 4d state surrounding of Fermi level widely. On the other hand, the energy band gap, E_g, of Sr_2TiO_4 was determined between the O 2p state and Ti 3d state. The calculation results correspond to experimental results in which Sr_2RuO_4 and Sr_2TiO_4 exhibit metallic and insulating behavior, respectively. In addition, the electrical resistivities for the $Sr_2Ru_{1-x}Ti_xO_4$ solid solution as shown in Fig. 3 are also supported by both electric state diagrams. With increasing x, a band gap is induced to a shrunk the Ru 4d state and to expand the Ti 3d state. It is speculated that the change from metal to semi-conducting behavior of the $Sr_2Ru_{1-x}Ti_xO_4$ is due to the appearance of a band gap for in compositions $0.2 \leq x \leq 0.4$. In addition, the energy levels of the Sr and O orbitals are elevated due to the substitution of Ti^{4+} for Ru^{4+}.

4. Conclusion

The lattice constants of the $Sr_2Ru_{1-x}Ti_xO_4$ solid solution refined by the WPPD method exhibit an increased a-axis and decreased c-axis with the substitution of Ti^{4+} for Ru^{4+}. The change from metal to semi-conducting behavior for the $Sr_2Ru_{1-x}Ti_xO_4$ was confirmed between $x = 0.2$ and 0.4. Compounds of the $Sr_2Ru_{1-x}Ti_xO_4$ with $x = 0$, 0.2, 0.4, 0.6 and 0.8 were confirmed to be p-type conductors by measurement of the Seebeck coefficient. Large difference of Seebeck coefficient was observed below 326.84 °C between $x = 0.4$ and 0.6. The first-principles molecular orbital (MO) calculations by DV Xα method were used for supporting electrical resistivity measurements.

Acknowledgment

A part of this study was supported by the NITECH 21st Century COE program "World Ceramics Center for Environmental Harmony", "NIT-Seto Ceramics R&D Project".

References

1. Rao, C. N. R., Gangly, P., Singh, K. K. and Ram, R. A. M., A comparative study of the magnetic and electrical properties of perovskite oxides and the corresponding two-dimensional oxides of K_2NiF_4 structure. *J. Solid State Chem.*, 1988, **72**, 14–23.
2. Matsuura, T., Tabuchi, J., Mizusaki, J., Yamauchi, S. and Fueki, K., Electrical properties of $La_{2-x}SrCoO_4$. Part I. Structure, electrical conductivity, and Seebeck coefficient of single crystals ($x = 0, 0.5, 1.0$ and 1.5). *J. Phys. Chem.*, 1988, **49**(12), 1403–1408.
3. Tilley, R. J. D., Perovskites: materials for all seasons. *Endeavor*, 1990, **14**(3), 124–128.
4. Gangly, P. and Rao, C. N. R., Crystal chemistry and magnetic properties of layered metal oxides possessing the K_2NiF_4 or related structures. *J. Solid State Chem.*, 1984, **53**(2), 193–216.
5. Maeno, Y., Hashimoto, H., Yoshida, K., Nishizaki, S., Fujita, T., Bednorz, J. G. and lichtenberg, F., Superconductivity in a layered perovskite without copper. *Nature (London)*, 1994, **372**(6506), 532–534.
6. Minakata, M. and Maeno, Y., Magnetic ordering in Sr_2RuO_4 induced by nonmagnetic impurities. *Phys. Rev. B*, 2001, **63**(18), 180504/1-4.
7. Kikugawa, N. and Maeno, Y., Non-Fermi-liquid behavior in Sr_2RuO_4 with nonmagnetic impurities. *Phys. Rev. Lett.*, 2002, **89**(11), 117001/1-4.
8. Oswald, H. R., Casagrande, S. F. and Reller, A., Structure and properties of perovskite-related Sr–Ru–Ti–O phases. *Solid State Ionics*, 1993, **63–65**, 565–569.
9. Cuffini, S. L., Macagno, V. A., Carbonio, R. E., Melo, A., Trollund, E. and Gautier, J. L., Crystallographic, magnetic, and electrical properties of $SrTi_{1-x}Ru_xO_3$ perovskite solid solutions. *J. Solid State Chem.*, 1993, **105**, 161–170.
10. Toraya, H., Whole-powder-pattern fitting without reference to a structural model: application to X-ray powder diffractometer data. *J. Appl. Crystallogr.*, 1986, **19**(6), 440–447.
11. Adachi, H., Tsukada, M. and Satoko, C., Discrete variational Xa cluster calculations. Part I. Application to metal clusters. *J. Phys. Soc. Jpn.*, 1978, **45**(3), 875–883.
12. Matsubara, I., Thermo electric property of Ru system complex oxides. *TEC 1999*, 1999, 80–81 (in Japanese).